

This is the peer reviewed version of the following article:

Polymerization of misfolded Z alpha-1antitrypin protein lowers CX3CR1 expression in human PBMCs.

Srinu Tumpara, Matthias Ballmaier, Sabine Wrenger, Mandy König, Matthias Lehmann, Ralf Lichtinghagen, Beatriz Martinez-Delgado, Elena Korenbaum, David DeLuca, Nils Jedicke, Tobias Welte, Malin Fromme, Pavel Strnad, Jan Stolk, Sabina Janciauskiene

Elife. 2021 May 18;10:e64881.

which has been published in final form at

<https://doi.org/10.7554/eLife.64881>

Polymerization of misfolded Z alpha-1antitrypsin protein lowers CX3CR1 expression in human PBMCs

Running title

Regulation of CX3CR1 by Z-alpha-1antitrypsin polymers

Srinu Tumpara¹, Matthias Ballmaier², Sabine Wrenger¹, Mandy König³, Matthias Lehmann³, Ralf Lichtinghagen⁴, Beatriz Martinez-Delgado⁵, Elena Korenbaum⁶, David DeLuca¹, Nils Jedicke⁷, Tobias Welte¹, Malin Fromme⁸, Pavel Strnad⁸, Jan Stolk⁹, Sabina Janciauskiene^{1,9}

¹Department of Respiratory Medicine, Hannover Medical School, Biomedical Research in Endstage and Obstructive Lung Disease Hannover (BREATH), Member of the German Center for Lung Research (DZL), Hannover 30625, Germany

²Cell Sorting Core Facility, Hannover Medical School, Hannover 30625, Germany

³8sens.biognostic GmbH, Berlin 13125, Germany

⁴Institute of Clinical Chemistry, Hannover Medical School, Hannover 30625, Germany

⁵Department of Molecular Genetics, Institute of Health Carlos III, Center for Biomedical Research in the Network of Rare Diseases (CIBERER), Majadahonda 28220, Spain

⁶Institute for Biophysical Chemistry, Hannover Medical School, 30625 Hannover, Germany

⁷Department of Gastroenterology, Hepatology and Endocrinology, Hannover Medical School, Hannover 30625, Germany

⁸Medical Clinic III, Gastroenterology, Metabolic Diseases and Intensive Care, University Hospital RWTH Aachen, Aachen 52074, Germany.

⁹Department of Pulmonology, Leiden University Medical Center, Leiden 2333, Netherlands; Member of European Reference Network LUNG, section Alpha-1-antitrypsin Deficiency

Corresponding author:

Prof. Dr. Sabina Janciauskiene

Hannover Medical School, Department of Respiratory Medicine

Feodor-Lynen Str. 23, 30625 Hannover, Germany

Tel: +49-511-532-7297

e-mail: Janciauskiene.sabina@mh-hannover.de

Abstract

The CX3CR1 (chemokine (C-X3-C motif) receptor 1) expression levels on immune cells have significant importance in maintaining tissue homeostasis under physiological and pathological conditions. The factors implicated in the regulation of CX3CR1 and its specific ligand CX3CL1 (fractalkine) expression remain largely unknown. Recent studies provide evidence that host's misfolded proteins occurring in the forms of polymers or amyloid fibrils can regulate CX3CR1 expression. Herein, a novel example demonstrates that polymers of human ZZ alpha-1 antitrypsin (Z-AAT) protein, resulting from its conformational misfolding due to the Z (Glu342Lys) mutation in *SERPINA1* gene, strongly lower CX3CR1 mRNA expression in human PBMCs. This parallels with increase of intracellular levels of CX3CR1 and Z-AAT proteins. Presented data indicate the involvement of the CX3CR1 pathway in the Z-AAT-related disorders and further support the role of misfolded proteins in CX3CR1 regulation.

Key words:

Alpha-1 antitrypsin/CX3CR1/CX3CL1/CD14/LPS/PBMCs/polymers/inflammation

Introduction

Interactions between the chemokine receptors and chemokines, but also other proteins, peptides, lipids, and microbial products, play a critical role in the recruitment of inflammatory cells into injured/diseased tissues¹. Many human diseases involve altered surface expression of chemokine receptors, which can lead to a defective cell migration and inappropriate immune response. Most of the human PBMCs express CX3CR1², also known as the G-protein coupled receptor 13 (GPR13) or fractalkine receptor, a mediator of leukocyte migration and adhesion. In the central nervous system, CX3CR1 is largely expressed by microglial cells (brain macrophages)³, which are involved in neurodegenerative diseases like Alzheimer's disease. The major role of CX3CR1-expressing cells is to recognize and enter tissue following CX3CL1 (fractalkine or also called neurotactin) gradient, and to crawl or "patrol" in the lumen of blood vessels⁴. Since CX3CR1/CX3CL1 axis is also involved in the synthesis of anti-inflammatory cytokines and has a significant role in cytoskeletal rearrangement, migration, apoptosis and proliferation, its dysregulation is associated with the development of cardiovascular diseases, kidney ischemia–reperfusion injury, cancer, chronic obstructive pulmonary disease (COPD), neurodegenerative disorders and others⁵⁻⁷. Some studies indicate that CX3CR1 deficiency contributes to the severity of infectious diseases⁸, and promotes lung pathology in respiratory syncytial virus-infected mice⁹. Animals with deletion of CX3CR1 show impaired phagocytosis¹⁰, which is a vital to prevent unwanted inflammation. It is clear that CX3CR1 expressing cells have tissue-specific roles in different pathophysiological conditions. Nevertheless, a comprehensive knowledge on the regulation of CX3CR1 expression is still missing.

Current findings suggest that divergent proteins with a common propensity to form extracellular oligomers interact with chemokine receptors and affect their expression levels. For example, Alzheimer's peptide, A β , interacts with CX3CR1 and significantly reduces its

expression in cultured microglial cells and in Alzheimer's brain¹¹. Similarly, highly aggregated extracellular Tau protein binds to CX3CR1, promotes its internalization and reduces expression in microglial cells¹². In concordance, polymers of human Z alpha-1 antitrypsin (Z-AAT), resulting from protein misfolding due to the Z (Glu342Lys) mutation in *SERPINA1* gene, lower CX3CR1 mRNA in human PBMCs, which parallels with increased intracellular CX3CR1 and Z-AAT protein levels.

Results and Discussion

Inherited alpha-1 antitrypsin deficiency (AATD) is a rare genetic condition caused by *SERPINA1* gene mutations. Homozygous Z AATD mutation is the most clinically relevant among Caucasians (prevalence is about 1:2000-1:5000) that is characterized by low plasma levels of AAT protein (10-15% compared to the wild type, MM AAT, 1.3-2 g/L) and the presence of intracellular and circulating Z-AAT polymers¹³. The liver is the major producer of AAT, therefore the accumulation of Z-AAT polymers in hepatocytes is a marker for diagnosing AATD¹⁴. The intracellular Z-AAT polymers have also been identified in other AAT expressing cells like monocytes and macrophages¹⁵. The accumulation of polymers is harmful for AAT-producing cells, whereas the circulating Z-AAT polymers are not able to execute the tasks of AAT protein, a major inhibitor of serine proteases having a strong immunomodulatory potential. Based on the facts that: i) circulating Z-AAT polymers contribute to the risk of developing pathologies^{16,17}, ii) pathogenic oligomeric proteins affect CX3CR1 expression¹² and iii) CX3CR1/CX3CL1 axis plays a significant role in immunity¹⁸, we aimed to investigate CX3CR1 expression in PBMCs of ZZ AATD individuals. For this, in collaboration with German Alpha1 Patient Association and Aachen University, was prepared RNA from freshly isolated PBMCs of 41 clinically stable ZZ AATD volunteers independently of their clinical diagnosis or treatment with intravenous AAT, a specific augmentation therapy¹⁹. For comparison, PBMCs isolated from healthy volunteers having normal plasma AAT levels were used. Additionally, a limited amount of RNA sample was

available from PBMCs isolated from a cohort of 12 ZZ AATD emphysema patients at Leiden University Medical Center, The Netherlands (**Figure 1–figure supplement 1**).

Independent of individual's age, clinical diagnosis (healthy, lung or liver disease) or augmentation therapy, the *CX3CR1* mRNA expression turned to be much lower in ZZ AATD PBMCs than in PBMCs from non-AATD controls [median (range): 4.1 (2.7-5.5) vs 18.5 (13-26.6), $p < 0.001$] (**Figure 1A**). A previous study has shown that *CX3CR1*^{-/-} mice have significantly higher plasma levels of CX3CL1 than wild-type mice²⁰. A diminished expression of CX3CR1 might be related to increased levels of soluble CX3CL1, an exclusive ligand for CX3CR1¹. However, the concentration of plasma CX3CL1 was low, and did not differ between ZZ AATD and non-AATD individuals (**Figure 1B**), and did not correlate with *CX3CR1* mRNA in PBMCs. The expression and release of CX3CL1 is generally low in the absence of inflammatory insults²¹ showing that at the time point of blood donation all volunteers were under stable clinical condition.

Although CX3CR1 is preferentially expressed on monocytes, other cells also express this receptor²². Previous reports indicated that exogenous IL-15 is a negative regulator of CX3CR1 expression in human CD56⁺ NK cells^{23,24}. However, plasma levels of IL-15 were lower in ZZ AATD than in non-AATD [pg/ml, median (range): 6.6 (5.9-6.9), $n = 23$ vs 7.63 (6.63-8.1), $n = 21$, $p = 0.001$], excluding a possible link between IL-15 and *CX3CR1* mRNA.

Because ZZ AATD individuals, differently from non-AATD, have about 90% lower blood concentration of Z-AAT protein, which may influence cellular microenvironment²⁵, a relationship between *CX3CR1* and Z-AAT plasma levels cannot be excluded. However, no correlation was found between *CX3CR1* mRNA in PBMCs and plasma levels of Z-AAT measured by nephelometry (data not shown). Next, plasma Z-AAT polymers were measured, as the biomarkers of all carriers of the Z allele^{13,26}. As anticipated, only minor amounts of polymers were detected in plasma of non-AATD individuals while plasma of ZZ AATD

contained high amounts of polymers [$\mu\text{g/ml}$, mean (SD): 4.1 (6), $n = 18$ vs 1399.8 (750), $n = 20$, respectively]. Since most of the ZZ AATD individuals received intravenous augmentation therapy with plasma purified AAT protein, ZZ AATD individuals were segregated into subgroups who receive or not receive therapy. There were no significant differences in Z-AAT polymer levels between the subgroups: [$\mu\text{g/ml}$, median (range): non-augmented 1506.6 (854-1781), $n = 17$ vs augmented 1348.5 (779.5-1529), $n = 23$, respectively]. A previous study used a sandwich ELISA based on 2C1 antibody and found that circulating Z-AAT polymers range between 8.2-230.2 $\mu\text{g/ml}$ in ZZ AATD¹³ whereas much higher circulating levels of Z-AAT polymers were detected by using the single monoclonal antibody (LG96)-based ELISA. These discrepancies can be due to the differences between antibody specificities. For example, 2C1 showed high affinity for polymers formed by heating M- or Z-AAT at 60°C²⁷ while LG96 antibody recognizes naturally occurring/native Z-AAT polymers without requiring sample heating. To answer, why some individuals have higher plasma levels of Z-AAT polymers than monomers (measured by nephelometry) is of great importance for the further studies.

Most interestingly, in ZZ-AATD individuals was found a trend towards an inverse relationship between *CX3CR1* mRNA in PBMCs and plasma Z-AAT polymers ($r^2 = -0.31$, $n = 38$, $p = 0.055$) (**Figure 1C**). This latter finding prompted more extensive investigation whether Z-AAT polymers affect *CX3CR1* expression when added to healthy donor PBMCs for 18 h, *ex vivo*. Lipopolysaccharide (LPS, from *Escherichia coli*, 1 $\mu\text{g/mL}$) was included as a known reducer of *CX3CR1* expression^{28,29}. Indeed, polymeric Z-AAT in a concentration-dependent manner lowered *CX3CR1* mRNA (**Figure 2–figure supplement 2**) whereas repeated experiments using Z-AAT at a constant concentration of 0.5 mg/mL reduced *CX3CR1* mRNA more than twice as compared to non-treated controls (**Figure 2A**). In accordance, LPS and polymer containing Z-AAT preparation significantly decreased surface expression of *CX3CR1*, specifically in CD14^+ monocytes and NK cells (**Figure 3**).

By contrast, cellular levels of CX3CR1 protein increased in PBMCs treated with Z-AAT polymers or LPS (used as a positive control) as compared to non-treated controls (**Figure 2B**). The CX3CR1 protein was present in detergent resistant lipid raft fraction of PBMCs treated with Z-AAT (**Figure 2-figure supplement 3A**). Total cell lysates and lipid raft fractions from Z-AAT-treated PBMCs, in contrast to those prepared from M-AAT-treated or non-treated PBMCs, contained high amounts of AAT polymers (**Figure 2C, figure 2-figure supplement 3B**). The laser scanning confocal microscopy of double-labelled specimens showed a co-localization of Z-AAT polymers with CX3CR1 protein (**Figure 2D**). Furthermore, 3D reconstruction of cross-sections visualised larger Z-AAT aggregates surrounded by cellular extensions in a cap-like formation, suggesting that cells may react differently depending on the size of Z-AAT polymers (**Figure 2E**). It cannot be excluded, that Z-AAT polymers, similar like polymers of Tau protein, interact with CX3CR1 and get internalized³⁰. This may determine the fate of CX3CR1 mRNA expression, i.e. sequestered intracellularly and not returning to the cell surface, CX3CR1 protein may induce signalling pathways lowering *CX3CR1* expression. To achieve a definitive answer how Z-AAT or other types of protein polymers regulate CX3CR1 levels detailed mechanistic studies are required. In general, along with transcriptional regulation, chemokine receptors trafficking is of great importance to understand³¹.

Under the same experimental conditions, monomeric M-AAT had no effect on CX3CR1 mRNA [expression relative to housekeeping gene HPRT1, mean (SD): 24.9 (2.9) controls, n = 5 vs 23.7 (1.3), n = 5, NS], and protein levels (**Figure 2B**). Likewise, monomeric Z-AAT protein does not affect CX3CR1 mRNA and protein levels, and heat-induced polymers of M-AAT showed no effect on CX3CR1 expression as well (**Figure 2-figure supplement 4**). Probably, specific conformational properties and/or molecular sizes of Z-AAT polymers are required for their interaction with CX3CR1. For example, cell surfaces express CX3CL1 as a constitutive oligomer (three to seven molecules), which is essential for efficient interaction

176 with CX3CR1^{32,33}. Numerous chemokines tend to self-associate that determines their
177 activity³⁴, and therefore certain Z-AAT polymers may resemble chemokine structures
178 competing for the same receptor(s). In some experimental models, Z-AAT polymers
179 expressed strong chemotactic properties^{16,35}. When chemokine receptors are engaged in
180 chemotaxis, they can be removed from the cell surface by the ligand-receptor
181 internalisation³⁶, which might explain a decrease of CX3CR1 in ZZ PBMCs. Interestingly,
182 the soluble form of CX3CL1, even when used at a high concentration of 500 ng/ml, does not
183 antagonize Z-AAT polymer effects on CX3CR1 mRNA and protein levels, and by itself
184 showed no effect on CX3CR1 mRNA or protein levels (**Figure 2-figure supplement 5**),
185 although some studies reported that CX3CL1 reduces CX3CR1 expression^{28,37}. In solution
186 CX3CL1 remains monomeric, even at high concentrations^{32,38} whereas, as mentioned above,
187 membrane bound CX3CL1 occurs as oligomer. These two forms of the CX3CL1 perform
188 differential roles³⁹, and therefore it cannot be excluded that oligomeric, but not a soluble, form
189 of CX3CL1 would compete with Z-AAT for CX3CR1 interaction *in vivo*.

190 The CX3CR1 helps to define the major subsets of human monocytes because classical
191 monocytes express much lower levels of CX3CR1 than non-classical monocytes⁴⁰. After *in*
192 *vitro* challenge with LPS for longer periods (like for 18 h), human monocytes are known to
193 increase in the mRNA and membrane expression of CD14, a receptor for LPS⁴¹. The
194 enhancement of CD14 expression after treatment of PBMCs with Z-AAT strikingly
195 resembled LPS (**Figure 4** and **Figure 4-figure supplement 1**). This raised a suspicion that Z-
196 AAT preparations might contain endotoxin. According to the Limulus Amebocyte Lysate
197 Test (LAL), endotoxin levels of Z-AAT preparations were below detection limit (0.01
198 EU/ml). Moreover, LPS significantly induced expression of TNF α , IL-6 and IL-1 β while
199 polymer containing Z-AAT preparations had no effect (**Figure 4-figure supplement 2**).
200 Beside, LPS but not Z-AAT significantly increased release of cytokines [IL-1 β , pg/ml,
201 median (range): LPS 1342.9 (1008-1834) vs Z-AAT 3.2 (2.5-5.9) vs controls 2.5 (2.1-3.7), n

= 4 independent experiments; TNF α , ng/ml, mean (SD): LPS 19.5 (2.5) vs Z-AAT vs controls, undetectable, n = 4 and IL-6, ng/ml, median (range): LPS 15903.5 (14626-17262) vs Z-AAT 5.4 (2.9-6.1) vs control (1.7 (1.0-2.3), n = 4]. Therefore, the effect of Z-AAT preparations on CD14 is valid and unrelated to a potential LPS-contamination. Although both Z-AAT polymers and LPS induce CD14 expression and similarly affect CX3CR1 expression and protein levels, data imply that Z-AAT polymers and LPS do not share the same signalling mechanisms.

As a side note, it has been reported that CD14⁺⁺ monocytes have the lowest expression of CX3CR1⁴². Low and high surface CX3CR1 levels are suggested to delineate two functional subsets of murine blood monocytes: “inflammatory” and “resident monocytes,”⁴³. This dichotomy appears conserved in humans as CD14⁺ CD16⁻, and CD14^{low} CD16⁺ monocytes resemble “inflammatory” and “resident” monocytes. Previous study demonstrated that peripheral blood monocytes of clinically healthy young adults (30-year old) with ZZ AATD have significantly higher mRNA and surface expression of CD14 as compared to age matched MM subjects⁴⁴. Authors thought that the higher CD14 expression reflects early pathological processes whereas according to the current findings this phenomenon seems to relate with the circulating Z-AAT polymers.

During steady state, non-classical monocytes expressing CX3CR1 patrol healthy tissues through crawling on the resting endothelium but these monocytes are required for a rapid tissue invasion at the site of infection or inflammation^{45,46}. Previous work evidenced that the non-classical subset of monocytes, characterized by high expression of CX3CR1, is almost absent in ZZ AATD emphysema patients⁴⁷. Moreover, plasma levels of AAT polymers were found to correlate with the levels of endothelium-related markers like sE-selectin and sICAM-1⁴⁸. Beyond, in a small cohort of ZZ AATD emphysema patients was found a strong inverse association between lung function, based on percentage (%) predicted transfer factor for

carbon monoxide (TLCO%pred) and forced expiratory volume in 1 second (FEV1%pred), and plasma levels of Z-AAT polymers: [TLCO%pred ($r^2=-0.75$, $n=9$, $p=0.02$) and FEV1%pred ($r^2=-0.82$, $n=9$, $p=0.006$)]. Thus, higher levels of Z-AAT polymers and lower numbers of CX3CR1-positive cells may favour the development of lung injury and disease. A decrease in the expression of CX3CR1 on human monocytes has been shown in patients with atopic dermatitis⁴⁹, and septic²⁸.

To date, many functional aspects of the CX3CR1-CX3CL1 axis have been suggested, including the adhesion of immune cells to vascular endothelial cells, chemotaxis, the crawling of the monocytes that patrol on vascular endothelial cells, the retention of monocytes of the inflamed endothelium to recruit inflammatory cells, and the survival of the macrophage. Considering the above, these different aspects of interactions between PBMCs and Z-AAT or other polymers occurring due to genetic or post-translational protein modifications require further investigations in dedicated clinical and experimental studies.

Material and methods

Key Resources Table				
Reagent type (species) or resource	Designation	Source or reference	Identifiers	Additional information
Biological sample (Homo sapiens)	PBMCs	Blood samples		collected from 41 ZZ-AATD and 21 non-AATD healthy controls
sequenced-based reagent (human)	CX3CR1	Thermofisher Scientific	Taqman assay 4331182	Hs00365842_m1

sequenced-based reagent (human)	TNFA	Thermofisher Scientific	Taqman assay 4331182	Hs01113624_g1
sequenced-based reagent (human)	IL6	Thermofisher Scientific	Taqman assay 4331182	Hs00985639_m1
sequenced-based reagent (human)	IL1B	Thermofisher Scientific	Taqman assay 4331182	Hs01555410_m1
sequenced-based reagent (human)	HPRT1	Thermofisher Scientific	Taqman assay 4331182	Hs02800695_m1
sequenced-based reagent (human)	CD14	Thermofisher Scientific	Taqman assay 4331182	Hs00169122_g1
Other	non-adherent 12-well plates	Greiner Bio-One	665970	
Other	Alpha-1 Antitrypsin Select matrix	GE Healthcare Life Sciences, Cytiva	17547201	
Other	Plasma purified human AAT	CSL Behring	Respreeza	
Other	LPS	Sigma-Aldrich	L2880	Escherichia coli O55:B5
commercial assay or kit	Pierce Chromogenic Endotoxin Quant Kit	Thermofisher Scientific	A39553	

commercial assay or kit	UltraRIPA kit	BioDynamics Laboratory	F015	
antibody	anti-AAT polymer, LG96 (mouse monoclonal)	deposited at German Collection of Microorganisms and Cell Cultures: DSM ACC3092	LG96	Coating: 1 µg/ml; LG96-HRP conjugate: (1:2000)
antibody	anti-human AAT (rabbit polyclonal)	Agilent Dako	A001202-2	(1:800)
antibody	anti-AAT polymer (mouse monoclonal)	Hycult Biotech	Clone 2C1; HM2289	(1:500)
antibody	anti-CX3CR1 (rabbit polyclonal)	Abcam	ab8021	(1:500)
antibody	anti-β-actin (mouse monoclonal)	Sigma-Aldrich	Clone AC-15; A3854	HRP-conjugated; (1:20,000)
antibody	anti-CX3CR1 (rabbit polyclonal)	Abcam	ab8021	(1:500)
antibody	anti-CX3CR1 (mouse monoclonal)	Invitrogen, Thermofisher Scientific	Clone 2A9-1; 12-6099-42	PE-conjugated; 5 µl per test
antibody	anti-CD14 (mouse monoclonal)	Invitrogen, Thermofisher Scientific	Clone TuK4; MHCD1401	FITC-conjugated; 5 µl per test

antibody	anti-CD16 (mouse monoclonal)	Immunotools	clone 3G8; 21278166	APC- conjugated; 5 µl per test
antibody	anti-CD56 (mouse monoclonal)	BD Biosciences	Clone NCAM16.2; 566124	BV-480 conjugated; 5 µl per test
peptide, recombinant protein	Human CX3CL1/ Fractalkine	Biotechne	365-FR-025	
software, algorithm	FlowJo	Becton, Dickinson and Company		V10
software, algorithm	SigmaPlot 14	Systat Software		V14.0

241

242 *Study approval*

243 The study cohort consists of 41 clinically stable ZZ AATD volunteers collected in
244 collaboration with German Alpha1 Patient Association and Aachen University independently
245 on their clinical diagnosis or treatment with intravenous AAT and 21 non-AATD healthy
246 controls. The institutional review board of Aachen University (EK 173/15) provided ethical
247 approval for individuals recruited in Germany. For Z-AAT polymer determination, we added
248 12 ZZ AATD emphysema patients recruited at Leiden University Medical Center. In addition,
249 9 ZZ AATD emphysema patients (4 males and 5 female) were enrolled with mean (SD): age
250 51 (6.6) years, forced expiratory volume in 1 second percent predicted [FEV1%pred, 66.3
251 (28)] and transfer factor of the lung for carbon monoxide percent predicted (TLCO%pred, 64
252 (29)]. The plasma levels of Z-AAT polymers in these cases were median (range) 714.2
253 (412.9-2270.4) µg/mL). Leiden University Medical Center provided ethical approval (project
254 P00.083 and P01.101) for the additional study groups. For all individuals detailed medical
255 records data were anonymized. All participants issued a written informed consent according

to the ethical guidelines of the Helsinki Declaration (Hong Kong Amendment) as well as Good Clinical Practice (European guidelines).

Isolation of PBMCs

Total PBMCs were isolated from freshly obtained peripheral blood (within 6 hours) using Lymphosep (C-C-Pro, Oberdorla, Germany) discontinuous gradient centrifugation according to the manufacturer's instructions as described previously⁵⁰. Thereafter, cells were lysed with RLT buffer for RNA analysis or suspended in RPMI-1640 medium (Gibco, Thermofisher Scientific, Waltham, MA, USA) and plated into non-adherent 12-well plates (Greiner Bio-one, Kremsmünster, Austria) for the further analyses.

RT-PCR analysis

Isolation of total RNA, synthesis of cDNA and mRNA analysis using Taqman gene expression assays (Thermofisher Scientific, Waltham, MA, USA, **Table 1**) were performed as described previously⁵⁰. RT PCR was carried out in duplicates. RNA quality was checked on agarose gels.

Table 1. Primers for gene expression analysis

Primer	Assay ID
CX3CR1	Hs00365842_m1
TNFA	Hs01113624_m1
IL6	Hs00985639_m1
IL1B	Hs01555410_s1
HPRT1	Hs02800695_m1
CD14	Hs00169122_g1

AAT polymer ELISA

The AAT polymer ELISA using the monoclonal antibody LG96 (deposited under access No DSM ACC3092 at German Collection of Microorganisms and Cell Cultures) was developed by Candor Biosciences. Normal M-AAT was used for a negative control. Recovery ratio,

signal-to noise ratio, calibration curve, sample stability under different storage conditions were tested and all tests passed. A cross reactivity with M-AAT was not reported in any of the tests. Nunc MaxiSorp flat-bottom 96-well plates (Thermofisher, Waltham, MA, USA) were coated overnight at 2-8 °C with monoclonal antibody LG96, at 1 µg/ml in coating buffer pH 7.4 (Candor Biosciences, Wangen, Germany). After a 2 h blocking step, the plasma samples were applied in the previously determined dilutions made in LowCross-Buffer (Candor Biosciences), which also served as a blank. Incubation was performed for 2 h at RT. For detection, the captured antigen was incubated with antibody (LG96)-horseradish peroxidase (HRP) conjugate (1:2000) for 2 h. The conjugate was prepared in advance with the HRP Conjugation Kit Lightning-Link (Abcam, Cambridge, UK) according to the manufacturer's instructions. For signal development SeramunBlau fast2 microwell peroxidase substrate (Seramun, Heidesee, Germany) was used. The incubation was performed at room temperature for 12 minutes in the dark and the reaction was stopped with 2 M H₂SO₄. Plates were analyzed at 450 nm by microplate reader (Dynex Chantilly, VA, USA) equipped with Dynex Revelation 4.21 software. Measurements were carried out in triplicates.

Preparation of AAT proteins

Plasma M- and Z-AAT was isolated by affinity chromatography using the AAT specific Alpha-1 Antitrypsin Select matrix (GE Healthcare Life Sciences, Cytiva, Sheffield, UK) according to the manufacturer's recommendations. For Z-AAT preparation plasma from volunteers not receiving AAT augmentation therapy was pooled. To change the buffer in the M- and Z-AAT protein pools to Hank's balanced salt solution (HBSS, Merck, Darmstadt, Germany) Vivaspin centrifugal concentrators with 10,000 MWCO (Vivaproducts, Littleton, MA, USA) were used. Plasma purified human AAT (99% purity, Respreeza, Zemaira, CSL Behring, Marburg, Germany) was changed to HBSS by the same method. Protein concentrations were determined using Pierce BCA Protein Assay Kit (Thermofisher,

Waltham, MA, USA). The quality of the M- and Z-AAT preparations was confirmed on Coomassie gels (10% SDS PAGE, **Figure 2-figure supplement 1A**) and by analyzing endotoxin levels with Pierce Chromogenic Endotoxin Quant Kit according to the manufacturer's guidelines (ThermoFisher, Waltham, MA, USA) using TECAN Infinite M200 PRO (Männedorf, Switzerland). In both, M and Z-AAT preparations, endotoxin levels were below the detection limit (Assay sensitivity: 0.01-0.1 EU/ml).

Preparation of Z-AAT monomers

Z-AAT was isolated by affinity chromatography using AAT specific Alpha-1 Antitrypsin Select matrix as described above. After the isolation Z-AAT, protein was diluted with sterile 0.9% NaCl (Fresenius Kabi, Bad Homburg, Germany), and Vivaspin-20, 100 kDa centrifugal column units (Sartorius, Göttingen, Germany) were used to separate Z-AAT monomers from polymers. Protein concentrations were determined using the Pierce BCA Protein Assay Kit (ThermoFisher Scientific, Carlsbad, CA, USA) according to manufacturer's instructions. The Z-AAT protein monomers were confirmed by using 7.5% SDS-PAGE without sample heating and without β -mercaptoethanol (**Figure 2-figure supplement 1B**).

In vitro experiments with PBMCs from healthy donors

PBMCs (5×10^6 cells/ml) were incubated for 18 h at 37 °C, 5% CO₂ either alone, or with Z- or M-AAT proteins, or lipopolysaccharide (LPS, 1 μ g/mL, *Escherichia coli* O55:B5, Sigma-Aldrich, Merck, St. Louis, Missouri, USA). In some experiments, a recombinant CX3CL1 protein (R&D Systems, Bio-Techne, Minnesota, USA) was used. Protein was reconstituted at a concentration of 25 μ g/ml in sterile PBS containing 0.1% BSA (Sigma-Aldrich) and added to PBMCs at various concentrations up to 500 ng/ml either alone or together with Z-AAT (0.5 mg/ml) for 18 h. Afterwards, cells were used for RNA isolation, flow cytometry or Western blot analysis. For Western blot, PBMCs were lysed in RIPA buffer (Sigma-Aldrich), supplemented with protease inhibitor cocktail (Sigma-Aldrich). For some Western blot

experiments, we extracted detergent resistant lipid raft associated proteins from insoluble cell fractions using UltraRIPA kit according to the supplier's instructions (BioDynamics Laboratory, Tokio, Japan).

Western blot

Equal amounts of lysed proteins were separated by 7.5% or 10% SDS-polyacrylamide gels (under reducing conditions for CX3CR1 and non-reducing for total AAT or AAT polymer analysis) prior to transfer onto polyvinylidene difluoride (PVDF) membranes (Merck-Millipore, Burlington, MA, USA). Membranes were blocked for 1 h with 5% low fat milk (Carl Roth, Karlsruhe, Germany) followed by overnight incubation at 4 °C with specific primary antibodies: polyclonal rabbit anti-human AAT (1:800) (DAKO A/S, Glostrup, Denmark), mouse monoclonal anti-AAT polymer antibody (clone 2C1, 1:500, Hycult Biotech, Uden, The Netherlands), rabbit polyclonal anti-CX3CR1 (1:500, Abcam, Cambridge, UK), or HRP-conjugated monoclonal anti β -actin antibody (1:20,000, Sigma-Aldrich, Merck, St. Louis, Missouri, USA) for a loading control. The immune complexes were visualized with anti-rabbit or anti-mouse HRP-conjugated secondary antibodies (DAKO A/S) and enhanced by Clarity Western ECL Substrate (BioRad, Hercules, CA, USA). Images were acquired by using Chemidoc Touch imaging system (BioRad) under optimal exposure conditions and processed using Image Lab version 5.2.1. software (Bio-Rad). For quantification, the signal intensity of the CX3CR1 protein band in each lane was divided by the corresponding β -actin band intensity (normalization factor or loading control). Afterwards, the normalized signal of each lane was divided by the normalized target signal observed in the control sample to get the abundance of the CX3CR1 protein as a fold change relative to the control.

ELISA

Plasma samples from 22 ZZ-AATD and 21 non-AATD controls were analyzed for CX3CL1/Fractalkine using DuoSet kit (R&D systems, Minneapolis, MN, USA, assay sensitivity 0.072

ng/ml, detection range 0.2-10 ng/ml). Cell free culture supernatants were analyzed directly or stored at -80°C. ELISA Duoset kits for TNF- α (assay detection range 15.6-1000 pg/ml), IL-1 β /IL-1F2 (assay detection range 3.91-250 pg/ml), and IL-6 (assay detection range 9.38-600 pg/ml) were purchased from R&D Systems (Minneapolis, MN, USA) and were used according to the manufacturer's instructions. Plates were measured on Infinite M200 microplate reader (Tecan, Männedorf, Switzerland). Measurements were carried out in duplicates.

Flow cytometry analysis

PBMCs (2×10^6 cells per condition) were incubated with LPS (1 μ g/ml), M-AAT (1 mg/ml), or Z-AAT (0.5 mg/ml) for 18 h. Staining was performed with phycoerythrin (PE)-conjugated mouse monoclonal anti-CX3CR1 antibody (clone 2A9-1 Invitrogen, Thermofisher Scientific, Carlsbad, CA, USA), fluorescein (FITC)-conjugated mouse monoclonal anti-CD14 antibody (clone TuK4, Life technologies, Thermofisher Scientific, Carlsbad, CA, USA), allophycocyanin (APC)-conjugated mouse monoclonal anti-CD16 antibody (clone 3G8, Immunotools, Friesoythe, Germany), or BV-480 conjugated anti-CD56 mouse monoclonal antibody (Clone NCAM16.2, BD Biosciences, San Jose, CA, USA) alone or in combinations. Dead cells were excluded by a staining with 7-amino-actinomycin D (7-AAD). Samples were measured on a BD FACS Aria Fusion machine and analyzed with FlowJo v10 (Becton, Dickinson and Company, Franklin Lakes, NJ, USA). The gating strategy is shown in **Figure 3-figure supplement 1**.

Immunofluorescence Confocal Laser Microscopy

Human total PBMCs (2×10^6) were plated onto glass coverslips and incubated alone or with Z-AAT polymers (0.5 mg/ml) in RPMI medium for 18 h at 37°C and 5% CO₂. Cells were then washed with PBS, fixed with 3% paraformaldehyde in PBS for 20 min and continued with or without permeabilization with 0.5% Triton X-100 in PBS for 5 min at RT. For

immunolabeling, cells were co-incubated with primary antibodies against human CX3CR1 (rabbit polyclonal IgG (1:500), Abcam, Cambridge, UK) and anti-AAT polymer antibody, D11 (1:5000, mouse monoclonal) for 1 h, at RT. After washing, the cells were incubated with corresponding secondary antibodies (1:1000) conjugated to AlexaFluor-488 (goat anti-rabbit) or AlexaFluor-594 (goat anti-mouse) both from Thermo Fisher Scientific, Rockford, USA. After final wash, the cells were mounted on microscope slides using ProLong Gold Antifade Mountant with DAPI (Thermo Fisher Scientific, Carlsbad, CA, USA). Images were acquired using confocal laser microscope FluoView 1000 (Olympus, Shinjuku, Japan) equipped with a 60x oil immersion objective and differential interference contrast (DIC) in sequential mode. Confocal z-stacks were collected with a 0.25 μ m increment.

Statistics

Data were analyzed and visualized by using Sigma Plot 14.0. One-tailed Student's t-test was applied to compare two sample means on one variable. When more than two groups were involved in the comparison, one-way ANOVA was used. Data were presented as mean (SD). If normality test failed, the nonparametric Kruskal-Wallis one-way analysis or Mann-Whitney Rank Sum test was performed, and data were presented as median (range). For correlation analysis the Pearson's linear correlation method was used to measure the correlation for a given pair. A p-value of less than 0.05 was considered significant.

Acknowledgments

We thank the German society Alpha1 Deutschland e.V. and society members for support.

Additional information

Funding

This work was supported by the German Research Foundation grant STR 1095/6-1 (Heisenberg professorship, to P.S.), the Deutsche Forschungsgemeinschaft (DFG) consortium

SFB/TRR57 “Liver fibrosis” (to P.S. and C.T.), German Center for Lung Research (DZL) grant number 82DZL002A and the Stichting Alpha1 International Registry (AIR).

Author ORCIDs

Sabina Janciauskiene: <https://orcid.org/0000-0003-3228-8021>

Competing interests

TW reports personal fees from CLS Behring and Grifols and JS reports unrestricted grants from Kamada and CSL Behring, outside the submitted work. All remaining authors have declared no conflict of interest.

Ethics

The institutional review board of Aachen University (EK 173/15) provided ethical approval for individuals recruited in Germany. Leiden University Medical Center provided ethical approval (project P00.083 and P01.101) for the other study groups.

Additional files

Supplementary files

Source data and figure supplements are provided in supplementary file *Supplementary file Tumpara et al.*

References

1. Bachelierie, F. *et al.* International Union of Basic and Clinical Pharmacology. [corrected]. LXXXIX. Update on the extended family of chemokine receptors and introducing a new nomenclature for atypical chemokine receptors. *Pharmacol Rev* **66**, 1-79, doi:10.1124/pr.113.007724 (2014).

- 428 2. Bazan, J. F. *et al.* A new class of membrane-bound chemokine with a CX3C motif.
429 *Nature* **385**, 640-644 (1997).
- 430 3. Ransohoff, R. M. Chemokines and chemokine receptors: standing at the crossroads of
431 immunobiology and neurobiology. *Immunity* **31**, 711-721,
432 doi:10.1016/j.immuni.2009.09.010 (2009).
- 433 4. Auffray, C. *et al.* Monitoring of blood vessels and tissues by a population of monocytes
434 with patrolling behavior. *Science* **317**, 666-670, doi:10.1126/science.1142883 (2007).
- 435 5. Harrison, J. K. *et al.* Role for neuronally derived fractalkine in mediating interactions
436 between neurons and CX3CR1-expressing microglia. *Proc Natl Acad Sci U S A* **95**,
437 10896-10901, doi:10.1073/pnas.95.18.10896 (1998).
- 438 6. Ning, W. *et al.* Comprehensive gene expression profiles reveal pathways related to the
439 pathogenesis of chronic obstructive pulmonary disease. *Proc Natl Acad Sci U S A* **101**,
440 14895-14900, doi:10.1073/pnas.0401168101 (2004).
- 441 7. Rius, C. *et al.* Critical role of fractalkine (CX3CL1) in cigarette smoke-induced
442 mononuclear cell adhesion to the arterial endothelium. *Thorax* **68**, 177-186,
443 doi:10.1136/thoraxjnl-2012-202212 (2013).
- 444 8. Bonduelle, O., Duffy, D., Verrier, B., Combadiere, C. & Combadiere, B. Cutting edge:
445 Protective effect of CX3CR1+ dendritic cells in a vaccinia virus pulmonary infection
446 model. *J Immunol* **188**, 952-956, doi:10.4049/jimmunol.1004164 (2012).
- 447 9. Das, S. *et al.* Respiratory syncytial virus infection of newborn CX3CR1-deficient mice
448 induces a pathogenic pulmonary innate immune response. *JCI Insight* **2**,
449 doi:10.1172/jci.insight.94605 (2017).
- 450 10. Thome, A. D., Standaert, D. G. & Harms, A. S. Fractalkine Signaling Regulates the
451 Inflammatory Response in an alpha-Synuclein Model of Parkinson Disease. *PLoS One*
452 **10**, e0140566, doi:10.1371/journal.pone.0140566 (2015).

- 453 11. Cho, S. H. *et al.* CX3CR1 protein signaling modulates microglial activation and protects
454 against plaque-independent cognitive deficits in a mouse model of Alzheimer disease. *J*
455 *Biol Chem* **286**, 32713-32722, doi:10.1074/jbc.M111.254268 (2011).
- 456 12. Bolos, M. *et al.* Absence of CX3CR1 impairs the internalization of Tau by microglia.
457 *Mol Neurodegener* **12**, 59, doi:10.1186/s13024-017-0200-1 (2017).
- 458 13. Tan, L. *et al.* Circulating polymers in alpha1-antitrypsin deficiency. *Eur Respir J* **43**,
459 1501-1504, doi:10.1183/09031936.00111213 (2014).
- 460 14. Janciauskiene, S. M. *et al.* The discovery of alpha1-antitrypsin and its role in health and
461 disease. *Respir Med* **105**, 1129-1139, doi:10.1016/j.rmed.2011.02.002 (2011).
- 462 15. Belchamber, K. B. R., Walker, E. M., Stockley, R. A. & Sapey, E. Monocytes and
463 Macrophages in Alpha-1 Antitrypsin Deficiency. *Int J Chron Obstruct Pulmon Dis* **15**,
464 3183-3192, doi:10.2147/COPD.S276792 (2020).
- 465 16. Parmar, J. S. *et al.* Polymers of alpha(1)-antitrypsin are chemotactic for human
466 neutrophils: a new paradigm for the pathogenesis of emphysema. *Am J Respir Cell Mol*
467 *Biol* **26**, 723-730, doi:10.1165/ajrcmb.26.6.4739 (2002).
- 468 17. Strnad, P., McElvaney, N. G. & Lomas, D. A. Alpha1-Antitrypsin Deficiency. *N Engl J*
469 *Med* **382**, 1443-1455, doi:10.1056/NEJMra1910234 (2020).
- 470 18. Imai, T. & Yasuda, N. Therapeutic intervention of inflammatory/immune diseases by
471 inhibition of the fractalkine (CX3CL1)-CX3CR1 pathway. *Inflamm Regen* **36**, 9,
472 doi:10.1186/s41232-016-0017-2 (2016).
- 473 19. Janciauskiene, S. & Welte, T. Well-Known and Less Well-Known Functions of Alpha-1
474 Antitrypsin. Its Role in Chronic Obstructive Pulmonary Disease and Other Disease
475 Developments. *Ann Am Thorac Soc* **13 Suppl 4**, S280-288,
476 doi:10.1513/AnnalsATS.201507-468KV (2016).

- 477 20. Cardona, A. E. *et al.* Scavenging roles of chemokine receptors: chemokine receptor
478 deficiency is associated with increased levels of ligand in circulation and tissues. *Blood*
479 **112**, 256-263, doi:10.1182/blood-2007-10-118497 (2008).
- 480 21. Umehara, H. *et al.* Fractalkine in vascular biology: from basic research to clinical
481 disease. *Arterioscler Thromb Vasc Biol* **24**, 34-40,
482 doi:10.1161/01.ATV.0000095360.62479.1F (2004).
- 483 22. Landsman, L. *et al.* CX3CR1 is required for monocyte homeostasis and atherogenesis
484 by promoting cell survival. *Blood* **113**, 963-972, doi:10.1182/blood-2008-07-170787
485 (2009).
- 486 23. Barlic, J., Sechler, J. M. & Murphy, P. M. IL-15 and IL-2 oppositely regulate expression
487 of the chemokine receptor CX3CR1. *Blood* **102**, 3494-3503, doi:10.1182/blood-2003-
488 03-0946 (2003).
- 489 24. Sechler, J. M., Barlic, J., Grivel, J. C. & Murphy, P. M. IL-15 alters expression and
490 function of the chemokine receptor CX3CR1 in human NK cells. *Cell Immunol* **230**, 99-
491 108, doi:10.1016/j.cellimm.2004.10.001 (2004).
- 492 25. Ramos, M. V. *et al.* Interleukin-10 and interferon-gamma modulate surface expression
493 of fractalkine-receptor (CX(3)CR1) via PI3K in monocytes. *Immunology* **129**, 600-609,
494 doi:10.1111/j.1365-2567.2009.03181.x (2010).
- 495 26. Janciauskiene, S., Dominaitiene, R., Sternby, N. H., Piitulainen, E. & Eriksson, S.
496 Detection of circulating and endothelial cell polymers of Z and wild type alpha 1-
497 antitrypsin by a monoclonal antibody. *J Biol Chem* **277**, 26540-26546,
498 doi:10.1074/jbc.M203832200 (2002).
- 499 27. Miranda, E. *et al.* A novel monoclonal antibody to characterize pathogenic polymers in
500 liver disease associated with alpha1-antitrypsin deficiency. *Hepatology* **52**, 1078-1088,
501 doi:10.1002/hep.23760 (2010).

28. Pachot, A. *et al.* Decreased expression of the fractalkine receptor CX3CR1 on circulating monocytes as new feature of sepsis-induced immunosuppression. *J Immunol* **180**, 6421-6429, doi:10.4049/jimmunol.180.9.6421 (2008).
29. Sica, A. *et al.* Bacterial lipopolysaccharide rapidly inhibits expression of C-C chemokine receptors in human monocytes. *J Exp Med* **185**, 969-974, doi:10.1084/jem.185.5.969 (1997).
30. Chidambaram, H., Das, R. & Chinnathambi, S. Interaction of Tau with the chemokine receptor, CX3CR1 and its effect on microglial activation, migration and proliferation. *Cell Biosci* **10**, 109, doi:10.1186/s13578-020-00474-4 (2020).
31. Kershaw, T., Wavre-Shapton, S. T., Signoret, N. & Marsh, M. Analysis of chemokine receptor endocytosis and intracellular trafficking. *Methods Enzymol* **460**, 357-377, doi:10.1016/S0076-6879(09)05218-5 (2009).
32. Hermand, P. *et al.* Functional adhesiveness of the CX3CL1 chemokine requires its aggregation. Role of the transmembrane domain. *J Biol Chem* **283**, 30225-30234, doi:10.1074/jbc.M802638200 (2008).
33. Ostuni, M. A. *et al.* CX3CL1 homo-oligomerization drives cell-to-cell adherence. *Sci Rep* **10**, 9069, doi:10.1038/s41598-020-65988-w (2020).
34. Proudfoot, A. E. *et al.* Glycosaminoglycan binding and oligomerization are essential for the in vivo activity of certain chemokines. *Proc Natl Acad Sci U S A* **100**, 1885-1890, doi:10.1073/pnas.0334864100 (2003).
35. Lomas, D. A. & Mahadeva, R. Alpha1-antitrypsin polymerization and the serpinopathies: pathobiology and prospects for therapy. *J Clin Invest* **110**, 1585-1590, doi:10.1172/JCI16782 (2002).
36. Springer, T. A. Traffic signals for lymphocyte recirculation and leukocyte emigration: the multistep paradigm. *Cell* **76**, 301-314, doi:10.1016/0092-8674(94)90337-9 (1994).

37. White, G. E., McNeill, E., Channon, K. M. & Greaves, D. R. Fractalkine promotes human monocyte survival via a reduction in oxidative stress. *Arterioscler Thromb Vasc Biol* **34**, 2554-2562, doi:10.1161/ATVBAHA.114.304717 (2014).
38. Mizoue, L. S., Bazan, J. F., Johnson, E. C. & Handel, T. M. Solution structure and dynamics of the CX3C chemokine domain of fractalkine and its interaction with an N-terminal fragment of CX3CR1. *Biochemistry* **38**, 1402-1414, doi:10.1021/bi9820614 (1999).
39. Winter, A. N. *et al.* Two forms of CX3CL1 display differential activity and rescue cognitive deficits in CX3CL1 knockout mice. *J Neuroinflammation* **17**, 157, doi:10.1186/s12974-020-01828-y (2020).
40. Ziegler-Heitbrock, L. *et al.* Nomenclature of monocytes and dendritic cells in blood. *Blood* **116**, e74-80, doi:10.1182/blood-2010-02-258558 (2010).
41. Landmann, R. *et al.* Human monocyte CD14 is upregulated by lipopolysaccharide. *Infect Immun* **64**, 1762-1769 (1996).
42. Appleby, L. J. *et al.* Sources of heterogeneity in human monocyte subsets. *Immunol Lett* **152**, 32-41, doi:10.1016/j.imlet.2013.03.004 (2013).
43. Geissmann, F., Jung, S. & Littman, D. R. Blood monocytes consist of two principal subsets with distinct migratory properties. *Immunity* **19**, 71-82, doi:10.1016/s1074-7613(03)00174-2 (2003).
44. Sandstrom, C. S. *et al.* Endotoxin receptor CD14 in PiZ alpha-1-antitrypsin deficiency individuals. *Respir Res* **9**, 34, doi:10.1186/1465-9921-9-34 (2008).
45. Auffray, C., Sieweke, M. H. & Geissmann, F. Blood monocytes: development, heterogeneity, and relationship with dendritic cells. *Annu Rev Immunol* **27**, 669-692, doi:10.1146/annurev.immunol.021908.132557 (2009).

46. Cros, J. *et al.* Human CD14^{dim} monocytes patrol and sense nucleic acids and viruses via TLR7 and TLR8 receptors. *Immunity* **33**, 375-386, doi:10.1016/j.immuni.2010.08.012 (2010).
47. Stolk, J. *et al.* Blood monocyte profiles in COPD patients with PiMM and PiZZ alpha1-antitrypsin. *Respir Med* **148**, 60-62, doi:10.1016/j.rmed.2019.02.001 (2019).
48. Aldonyte, R., Eriksson, S., Piitulainen, E., Wallmark, A. & Janciauskiene, S. Analysis of systemic biomarkers in COPD patients. *COPD* **1**, 155-164, doi:10.1081/copd-120030828 (2004).
49. Echigo, T., Hasegawa, M., Shimada, Y., Takehara, K. & Sato, S. Expression of fractalkine and its receptor, CX3CR1, in atopic dermatitis: possible contribution to skin inflammation. *J Allergy Clin Immunol* **113**, 940-948, doi:10.1016/j.jaci.2004.02.030 (2004).
50. Frenzel, E. *et al.* Acute-phase protein alpha1-antitrypsin--a novel regulator of angiopoietin-like protein 4 transcription and secretion. *J Immunol* **192**, 5354-5362, doi:10.4049/jimmunol.1400378 (2014).

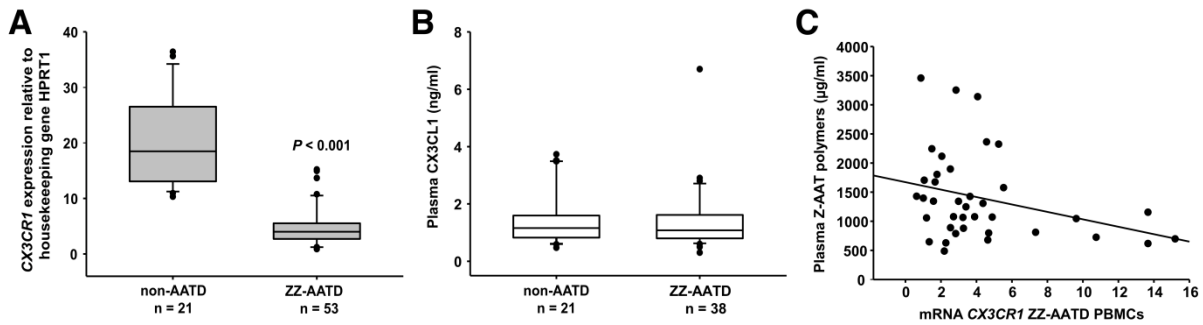


Figure 1. **A** *CX3CR1* gene expression in PBMCs isolated from AATD subjects and non-AATD controls. *CX3CR1* gene expression relative to *HPRT1* housekeeping gene was determined by real-time PCR using Taqman gene expression assays. Measurements were carried out in duplicates. Data are presented as median (IQR) in boxplots, lines represent medians. Outliers are defined as data points located outside the whiskers. p-value was calculated by the difference between the Mann-Whitney U test. **B** Plasma levels of CX3CL1 in AATD (plasma available for n = 38 AATD) and non-AATD individuals measured by ELISA. Measurements were carried out in triplicates. Data are presented as median (IQR) in boxplots with whiskers. Outliers are defined as data points located outside the whiskers. **C** Negative correlation of *CX3CR1* mRNA in PBMCs and plasma Z-AAT polymer levels from ZZ-AATD individuals from graph (B). Person's correlation test, $r^2 = -0.313$, $p = 0.055$, $n = 38$.

The online version of this article includes the following source data and figure supplement(s) for figure 1:

Figure 1—Source data 1. Source files, containing original data for Figure 1 **A** and **B**, to document CX3CR1 expression (**A**), and plasma levels of CX3CR1 in AATD and non-AATD individuals (**B**).

Figure 1—Figure supplement 1. Schematic presentation of the study design.

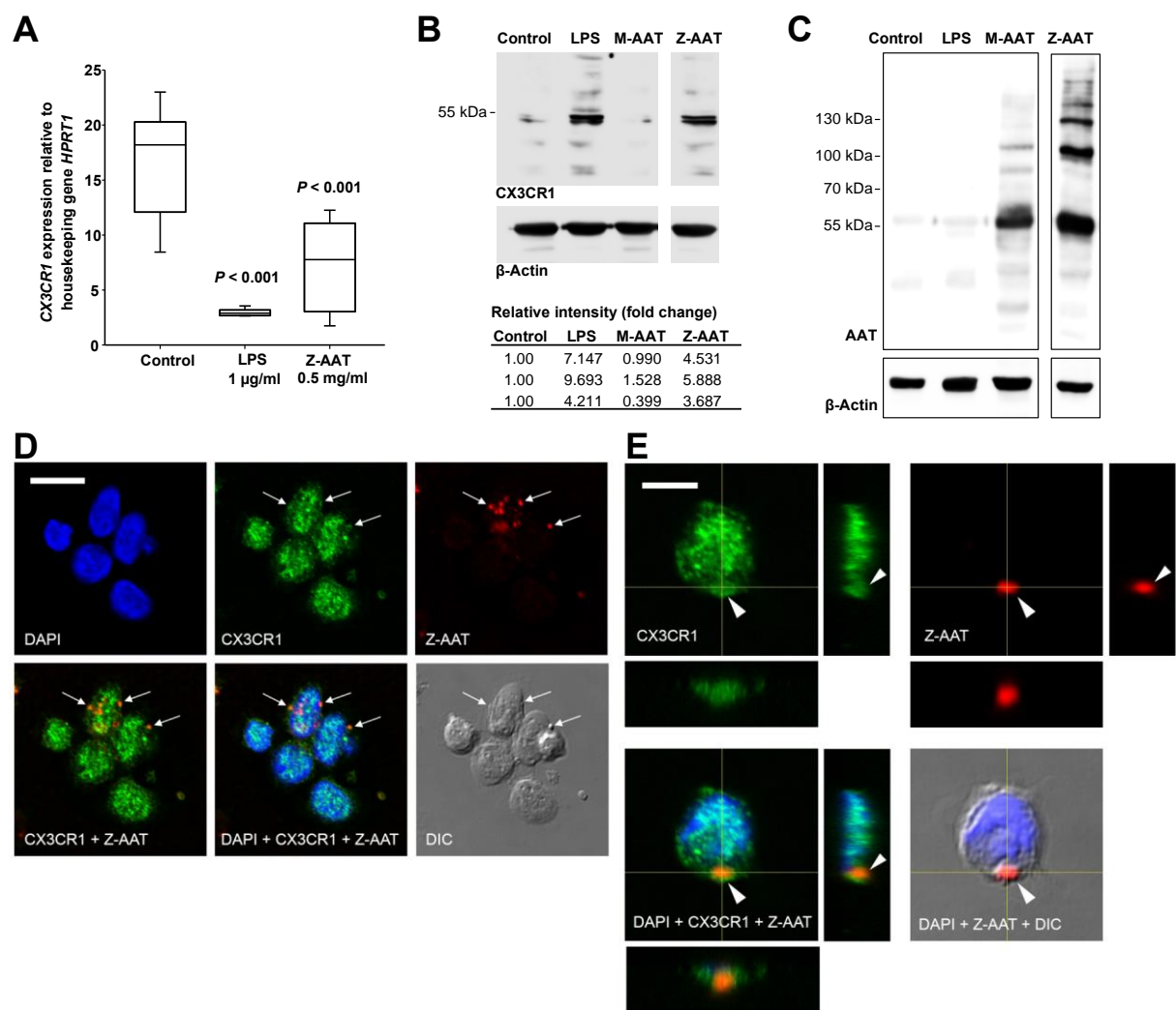


Figure 2. Effects of Z-AAT and M-AAT on CX3CR1 mRNA and protein expression. **A** *CX3CR1* gene expression relative to *HPRT1* housekeeping gene was determined by real-time PCR using Taqman gene expression assays. PBMCs were incubated for 18 h with plasma-derived Z-AAT, LPS or M-AAT in the concentrations as indicated, or with RPMI medium alone (control). The data from $n = 6$ independent experiments are presented as median (IQR) in box and whisker plot format; lines represent medians in each box. Measurements were carried out in duplicates. p was calculated by nonparametric Kruskal-Wallis test). **B** Representative uncut Western blot ($n = 3$ independent experiments) of CX3CR1 in RIPA lysates prepared from PBMCs incubated for 18 h alone or with LPS (1 µg/ml), M-AAT (1 mg/ml), or Z-AAT (0.5 mg/ml). For analysis of CX3CR1, equal amounts of protein were

separated by SDS-PAGE under reducing conditions. Relative intensities were calculated for each band using the ratio relative to β -actin, as a loading control, and then normalized by the experimental control. **C** For analysis of cellular AAT the same lysates were separated under non-reducing conditions. Western blots were probed with polyclonal rabbit anti human AAT recognizing monomeric, polymeric, or truncated forms of AAT. One representative blot from $n = 3$ independent experiments is shown. β -actin was used for a loading control. **D** and **E**. Co-distribution of Z-AAT polymers with CX3CR1 in human total PBMCs incubated with 0.5 mg/ml Z-AAT polymers for 18 h. **D** Immunofluorescence microscopy revealed co-localization of Z-AAT polymers (*red*) with CX3CR1-positive structures (*green*). Arrows point areas of co-localization. Scale bar, 10 μ m. **E** Confocal microscopy 3D-stack with orthogonal reconstruction shows an aggregate of Z-AAT polymers (*red*) surrounded by CX3CR1-positive (*green*) cellular extensions forming a cap-like structure (arrowhead). Scale bar, 5 μ m. The images with indicated channels merged and the corresponding DIC image are presented. DAPI was used for nuclei staining (*blue*).

The online version of this article includes the following source data for figure 2:

Figure 2—Source data 1. Source file, containing original data for Figure 2A, to document CX3CR1 reduced expression in PBMCs treated with Z-AAT or LPS (**A**).

Figure 2—Figure supplement 1. Quality control of isolated M- and Z-AAT proteins by SDS-PAGE.

Figure 2—Figure supplement 2. Z-AAT in a concentration-dependent manner reduces CX3CR1 mRNA expression in PBMCs isolated from healthy donors.

Figure 2—Figure supplement 3. Z-AAT induces association of CX3CR1 with lipid rafts.

Figure 2—Figure supplement 4. CX3CR1 transcript and protein expressions in presence of Z-AAT monomer, Z-AAT polymer, native M-AAT and M-AAT polymer.

624 **Figure 2—Figure supplement 5.** Effect of CX3CL1 alone or in combination with Z-AAT on
625 CX3CR1 transcript and protein expression.

626

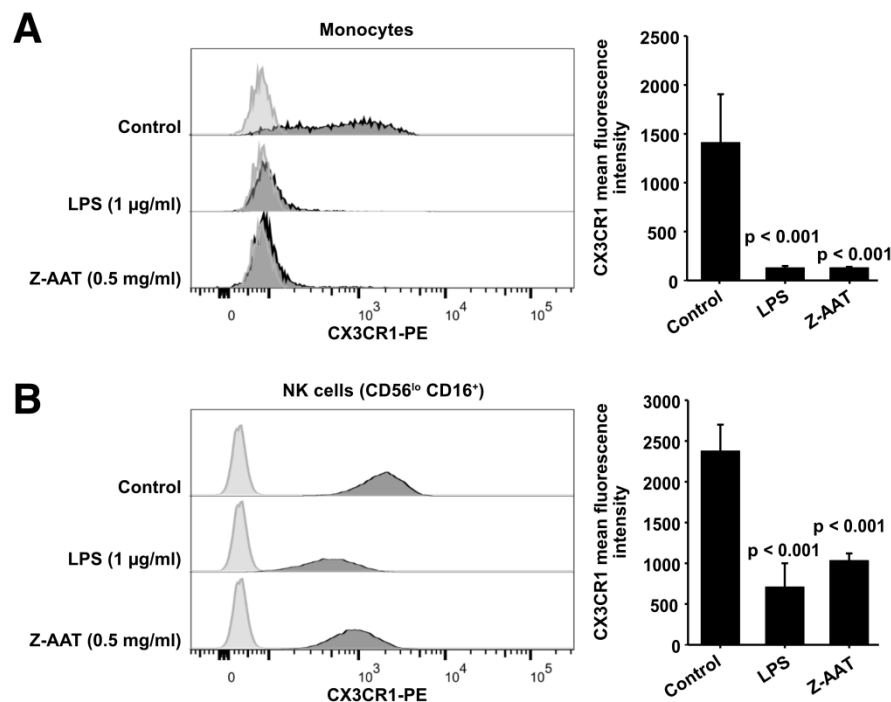
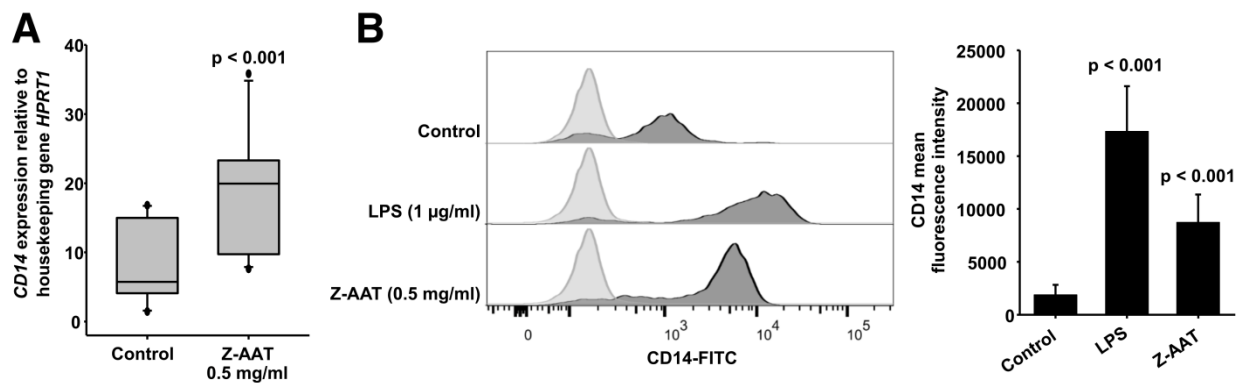


Figure 3. Flow cytometric analysis of CX3CR1 surface expression in PBMCs after incubation with RPMI alone (control), Z-AAT or LPS in the concentrations as indicated for 18 h. CX3CR1 expressing cells were found in the monocyte gate (**A**) and in the NK cell gate (CD56^{lo} CD16⁺) (**B**). Histograms show representative results and bars represent mean (SD) of n = 4 independent biological repeats each measured one time. After incubation with Z-AAT or LPS monocytes and NK cells show significantly reduced CX3CR1 surface expression in comparison to untreated control cells. p-values were calculated by one-way ANOVA.

The online version of this article includes the following source data and figure supplement(s) for figure 3:

Figure 3—Source data 1. Source files, containing original data for Figure 3A,B to document reduced CX3CR1 surface expression monocytes (**A**) and NK cells (**B**) after treatment with Z-AAT or LPS (**A**).

Figure 3—Figure supplement 1. Gating strategy: Sequential gating to identify monocytes and NK cells from total PBMCs.



643

644 **Figure 4.** Z-AAT and LPS induce CD14 expression. **A** Z-AAT increases *CD14* gene
645 expression. PBMCs were incubated for 18 h with 0.5 mg/ml Z-AAT or RPMI medium alone
646 (control). *CD14* mRNA expression relative to HPRT1 was determined by real-time PCR
647 using Taqman gene expression assays. Measurements were carried out in duplicates. Data are
648 represented as median (IQR) in boxplots, lines represent medians of n = 14 independent
649 biological repeats. Outliers are defined as data points located outside the whiskers. p-values
650 were calculated using nonparametric Kruskal-Wallis test.

651 **B** Z-AAT increases monocyte CD14 surface expression. PBMCs were cultured with RPMI
652 (control), Z-AAT or LPS for 18 h. CD14 mean fluorescence intensities of monocytic cells
653 were determined by flow cytometry. Histograms show representative results and bars
654 represent mean (SD) of n = 4 independent biological repeats each measured one time. p-
655 values were calculated from ANOVA.

656 The online version of this article includes the following source data and figure supplement(s)
657 for figure 4:

658 **Figure 4—Source data 1.** Source files, containing original data for Figure 6 **A,B** to document
659 CD14 gene expression in PBMCs (**A**) and CD14 surface expression in monocytes (**B**).

660 **Figure 4—Figure supplement 1.** Inverse changes in *CD14* and *CX3CR1* gene expression in
661 PBMCs treated with rising concentrations of Z-AAT.

662 **Figure 4—Figure supplement 2.** Z-AAT doesn't induce cytokine expression. PBMCs were
663 treated with Z-AAT or LPS (used as a positive control) for 18 h.

664

Legends for supplementary figures

Figure 1–figure supplement 1. Schematic presentation of the study design. The German cohort comprises 41 ZZ-Alpha1 Antitrypsin deficient (AATD) volunteers irrespective of clinical status and medications. For control, we collected blood from 21 non-AATD volunteers with normal AAT blood levels. We prepared PBMCs for further gene expression analysis by real-time PCR and plasma for determination of Z-AAT polymers by nephelometry. The Leiden cohort consisting of 12 ZZ-AATD emphysema patients was used for gene expression analysis.

Figure 2–figure supplement 1. Quality control of isolated M- and Z-AAT proteins by SDS-PAGE. **A.** Plasma M- and Z-AAT was purified by affinity chromatography with AAT specific Alpha1 Antitrypsin Select matrix. Proteins were run on a 10 % SDS-PAGE gel and stained with Coomassie Blue G250. AAT (Respreeza) was added as a positive control. Gels were run for each protein preparations. One representative gel is shown. **B.** Z-AAT polymers were purified by affinity chromatography with AAT specific Alpha1 Antitrypsin Select matrix and monomeric Z-AAT was separated by using vivaspin-20, 100 kDa centrifugal column units. Z-polymers, Z-monomers and native AAT (as control) were run on a 10 % SDS-PAGE gel without sample heating and without β -mercaptoethanol, and stained with Coomassie Blue G250. Representative gel is shown.

Figure 2–figure supplement 2. Z-AAT in a concentration-dependent manner reduces *CX3CR1* mRNA expression in PBMCs isolated from healthy donors. PBMCs were incubated for 18 h with plasma-derived Z-AAT in the concentrations as indicated. *CX3CR1* gene expression relative to *HPRT1* housekeeping gene was determined by real-time PCR using Taqman gene expression assays. Curves show results from two independent experiments. Each point represents mean of two repeats.

Figure 2–figure supplement 3. Z-AAT induces association of CX3CR1 with lipid rafts. Lipid rafts were solubilized from membrane fractions with ULTRA RIPA kit. **a** For analysis of CX3CR1, equal amounts of protein were separated by SDS-PAGE under reducing conditions. One representative blot from n = 3 independent experiments is shown. **b** For analysis of lipid raft associated AAT polymers the same samples were separated under non-reducing conditions. The Western blot was probed with monoclonal antibody (2C1) recognizing polymeric AAT. One representative blot from n = 3 independent experiments is shown.

Figure 2–figure supplement 4. CX3CR1 transcript and protein expressions in the presence of Z-AAT monomer, Z-AAT polymer, native M-AAT and M-AAT polymer. **A** *CX3CR1* mRNA expression relative to *HPRT1* was determined by real-time PCR using Taqman gene expression assays. PBMCs were incubated for 18 h in RPMI medium alone or with addition of Z-AAT monomer or Z-AAT polymer (each 0.5 mg/ml), or LPS (1µg/ml) or native M-AAT (0.5 mg/ml). Measurements were carried out in duplicates. Data are represented as bars from four independent experiments. **B** Levels of CX3CR1 lysates prepared in RIPA buffer from PBMCs incubated for 18 h with RPMI (control) and with Z-AAT monomer (0.5 mg/ml) or LPS (1µg/ml) (used as a positive control). For analysis of CX3CR1, equal amounts of protein were separated by 10% SDS-PAGE under reducing conditions followed by western blotting. Representative uncut Western blot (n = 2 independent experiments) is shown. β-actin was used for a loading control. **C** CX3CR1 mRNA expression relative to HPRT1 was determined by real-time PCR using Taqman gene expression assays. PBMCs were incubated for 18 h in RPMI medium alone or with different concentrations of heat-induced M-AAT polymers (60°C, for 3h). Measurements were carried out in duplicates. Data are represented as curves from two independent donors.

Figure 2–figure supplement 5. Effect of CX3CL1 alone or in combination with Z-AAT on CX3CR1 transcript and protein expression. PBMCs were incubated for 18 h with CX3CL1 and Z-AAT polymers separately or in combination or with RPMI medium alone (control). **A** *CX3CR1* gene expression relative to *HPRT1* housekeeping gene was determined by real-time PCR using Taqman gene expression assays. The data from n = 8 independent experiments for control and 100 ng/ml CX3CL1 conditions and n = 4 for 500 ng/ml CX3CR1 conditions with or without Z-AAT are presented as mean (SEM). Measurements were carried out in duplicates. P values were calculated from one-way ANOVA test. **B** Levels of CX3CR1 in RIPA lysates prepared from PBMCs incubated for 18 h with RPMI (control) and with CX3CL1 (100 ng/ml) and Z-AAT (0.5 mg/ml) separately or in combination. For analysis of CX3CR1, equal amounts of protein were separated by SDS-PAGE under reducing conditions followed by western blotting. Representative uncut Western blot (n = 2 independent experiments) is shown. β -actin was used for a loading control.

Figure 2-figure supplement 5-Source data 1. Source file, containing original data for Figure 5A to document CX3CR1 gene expression in PBMC.

Figure 3–figure supplement 1. Gating strategy: Sequential gating to identify monocytes and NK cells from total PBMCs. PBMCs were stained with CD14, CD16 and CD56 in the presence of 7-amino-actinomycin D (7-AAD). Dead cells were excluded by 7-AAD. From the single cells, CD14⁺ cells with a mid-level of granularity (SSC mid) were further gated for a mid-level FSC to identify monocytes. For the identification of NK cells, CD56⁺ cells with a low-level of granularity (SSC low) were further selected by CD16. The above plots are representative for four different donors.

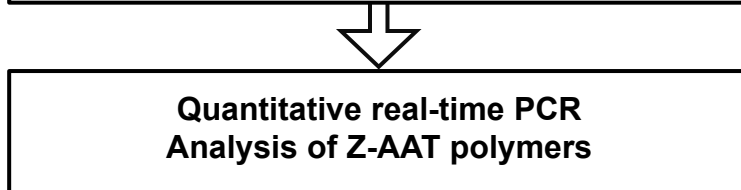
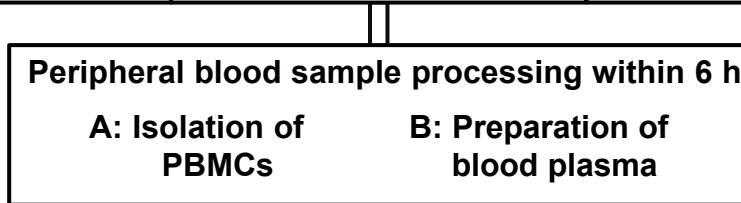
Figure 4–figure supplement 1. Inverse changes in *CD14* and *CX3CR1* mRNA expression in PBMCs treated with different concentrations of Z-AAT. PBMCs were incubated for 18 h with plasma-derived Z-AAT in the concentrations as indicated, or with RPMI medium alone

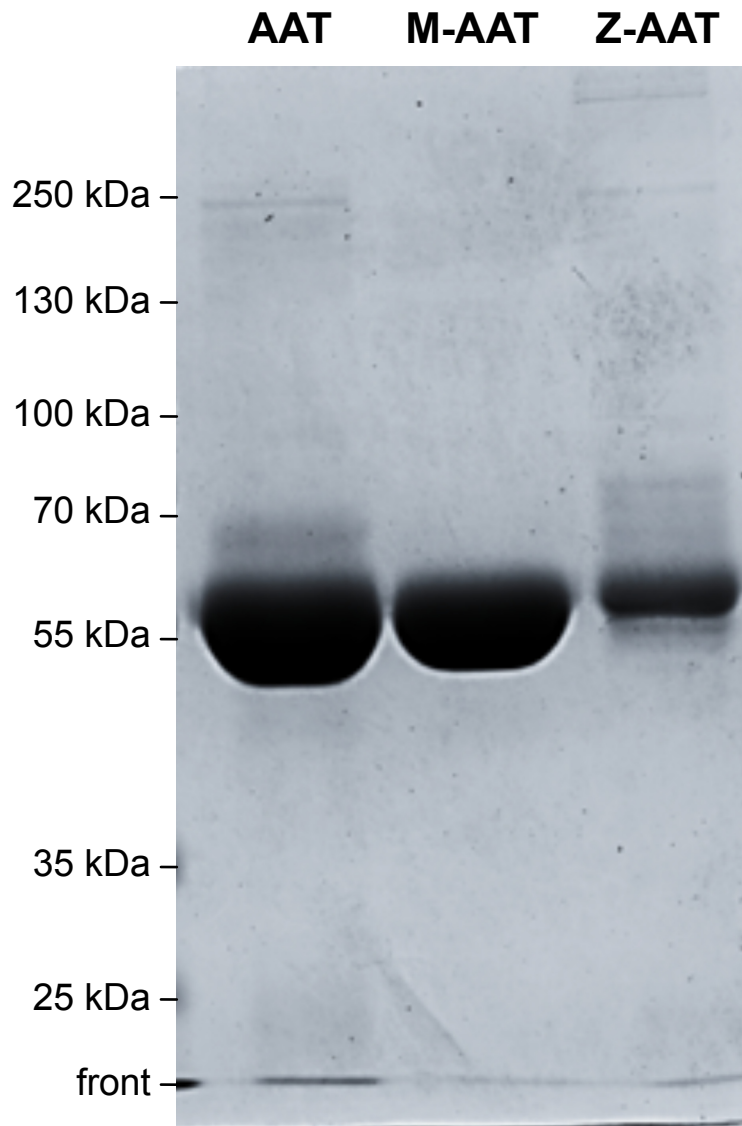
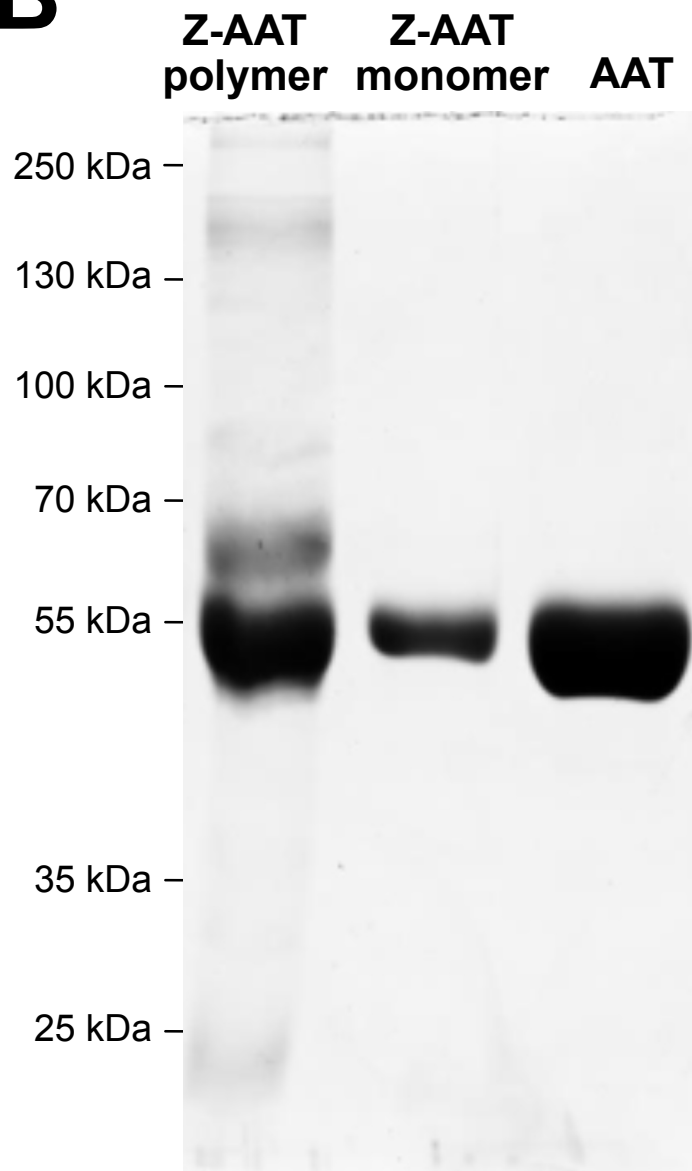
(control). *CX3CR1* and *CD14* gene expression relative to *HPRT1* housekeeping gene was determined by real-time PCR using Taqman gene expression assays. Curves represent two independent experiments.

Figure 4—figure supplement 2. Z-AAT doesn't induce cytokine expression. PBMCs were treated with Z-AAT or LPS (used as a positive control) for 18 h. *IL1B* (a), *IL6* (b) and *TNFA* (c) mRNA expression relative to *HPRT1* housekeeping gene was determined by real-time PCR using Taqman gene expression assays. Data presented as median (IQR) in box and whisker plots, lines represent medians, outliers are defined as data points located outside the whiskers. n = 4 independent experiments. p-values were calculated by Kruskal-Wallis one-way analysis.

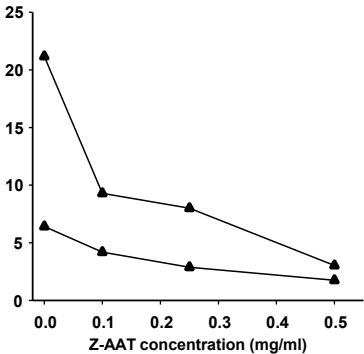
Figure 4—figure supplement 2—Source data 1. Source files, containing original data for Figure 4-figure supplement 2 to document *IL1B* (A), *IL6* (B) and *TNFA* (C) gene expression in PBMCs.

12 ZZ-AATD emphysema patients 6 females/6 males Age, median (range): 60 (41-70) years Plasma AAT, mean (SD): 0.3 (0.2) g/L	41 ZZ-AATD volunteers 21 females/20 males Age, median (range): 58 (43-80) years Plasma AAT, mean (SD): 0.91 (0.47) g/L	21 non-AATD volunteers 14 females/7 males Age, median (range): 42 (29-63) years Plasma AAT, mean (SD): 1.23 (0.35) g/L
---	---	---



A**B**

CX3CR1 expression relative to
housekeeping gene *HPRT1*

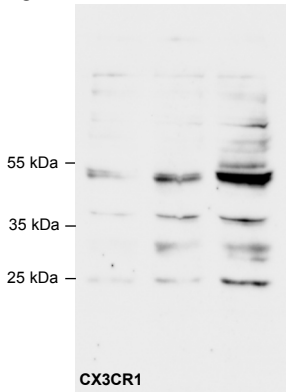


a

Control

M-AAT

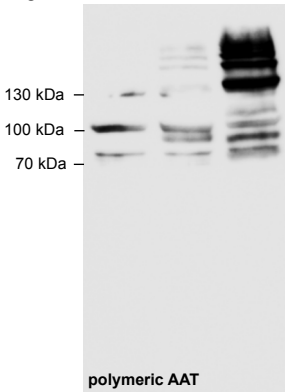
Z-AAT

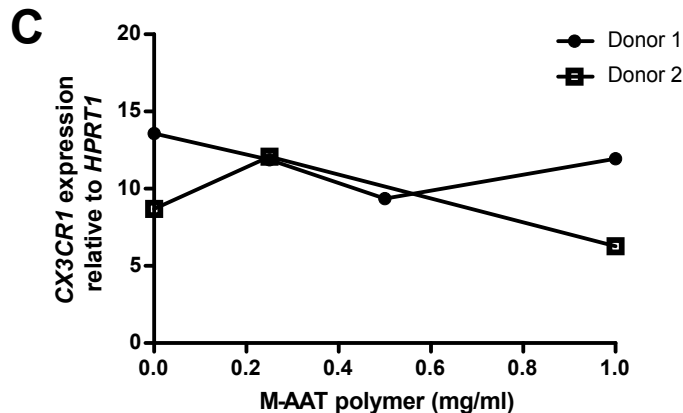
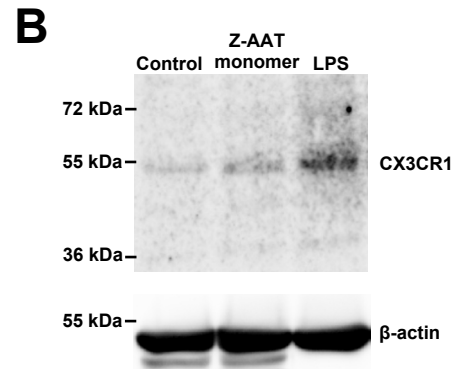
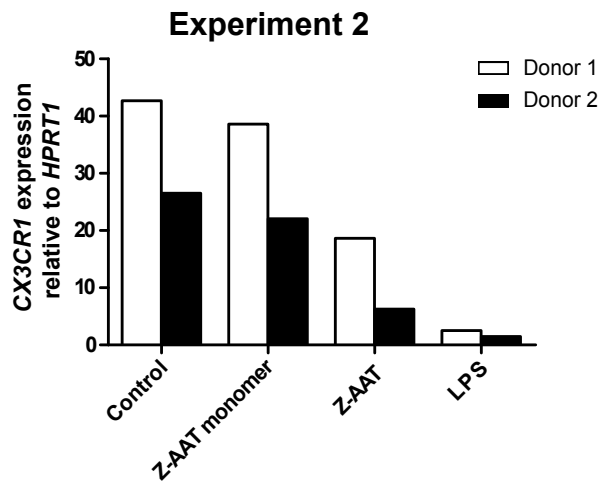
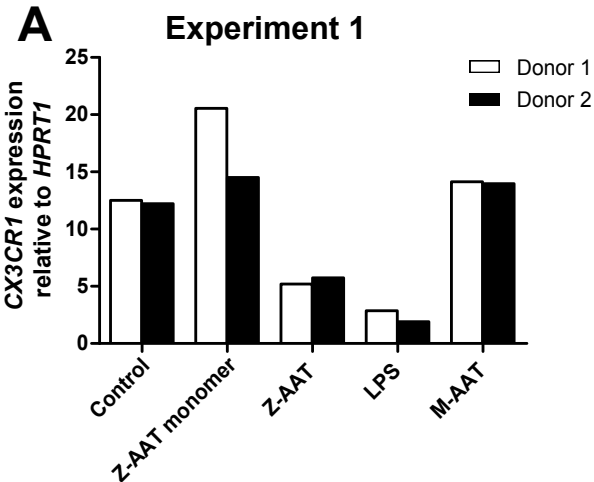
**b**

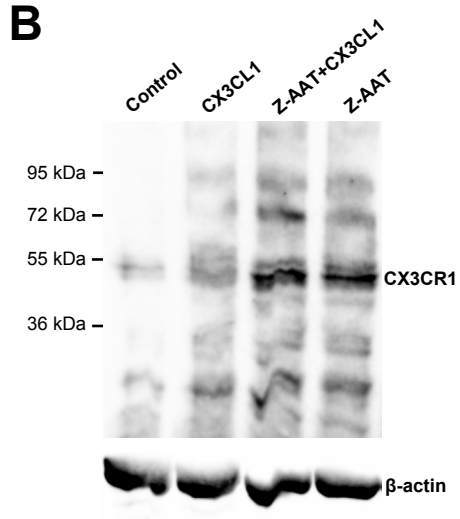
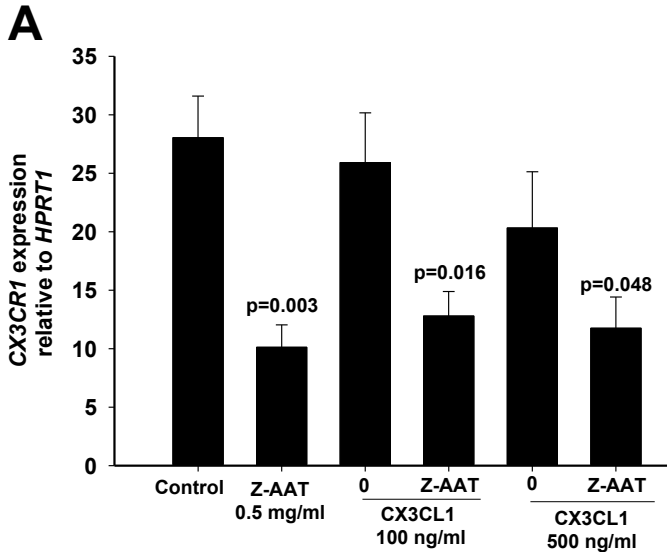
Control

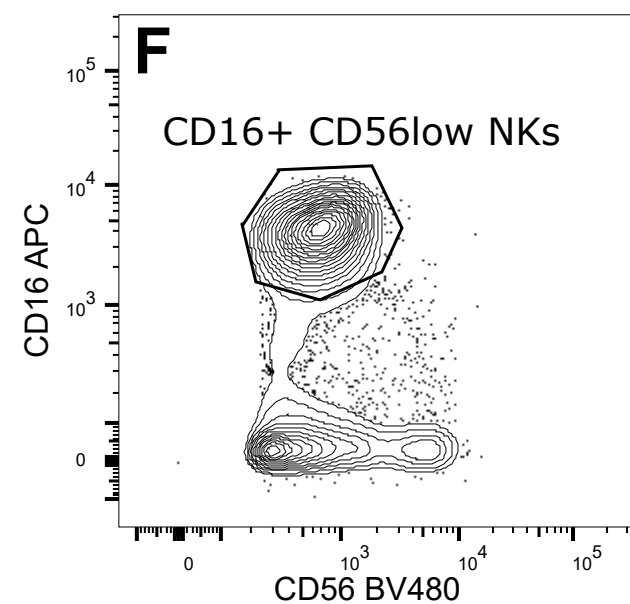
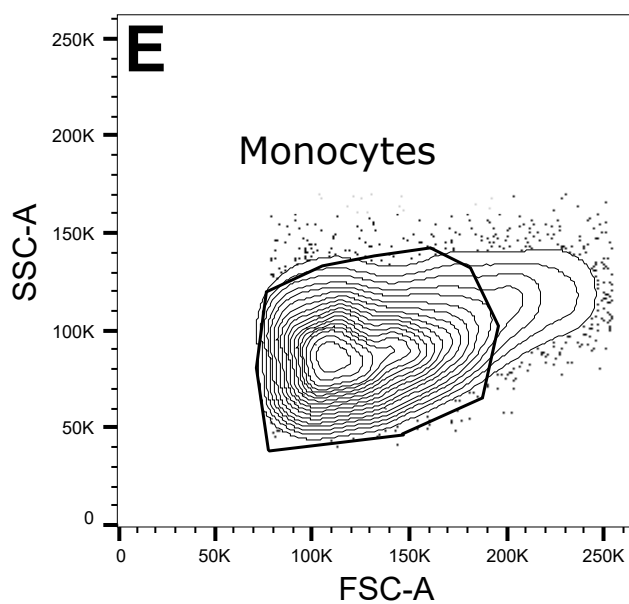
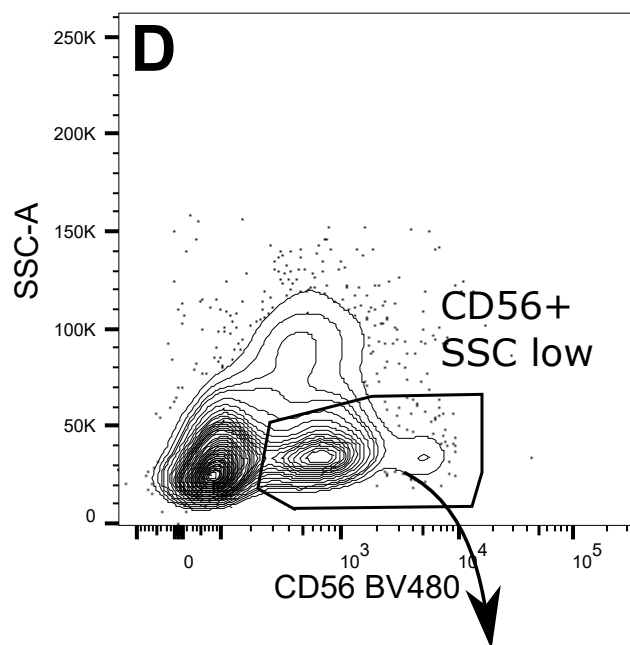
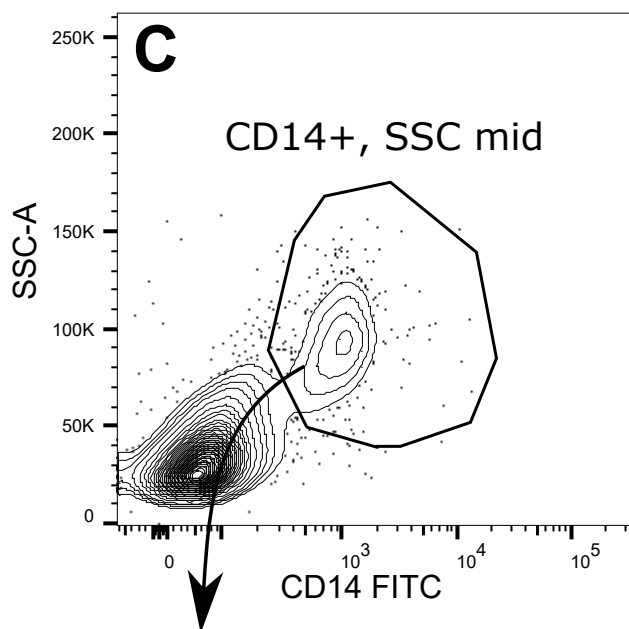
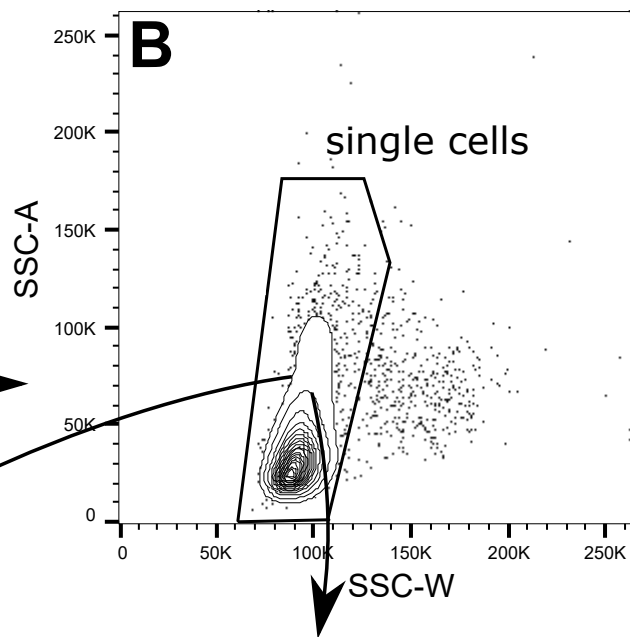
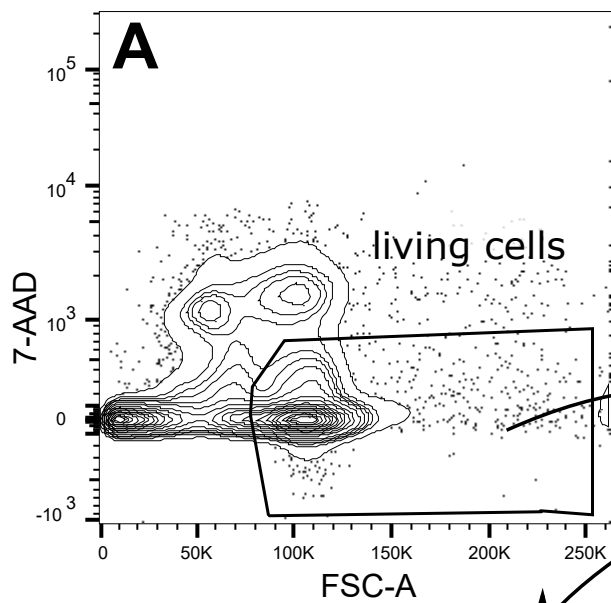
M-AAT

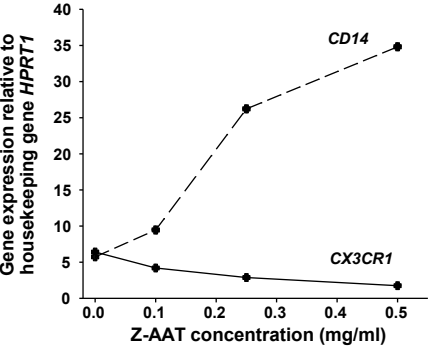
Z-AAT

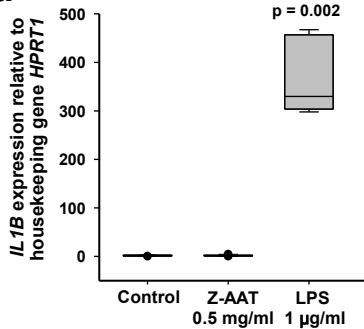
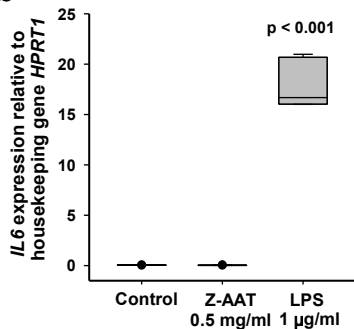










a**b****c**